# Mycelium-Enhanced Bacterial Degradation of Organic Pollutants under Bioavailability Restrictions

**Rungroch Sungthong,[†,‖] Margalida Tauler,[‡] Magdalena Grifoll,[‡] and Jose Julio Ortega-Calvo*[,†]**

[†]Instituto de Recursos Naturales y Agrobiología de Sevilla (IRNAS-CSIC), Apartado 1052, Seville 41080, Spain

[‡]Department of Genetics, Microbiology and Statistics, Faculty of Biology, University of Barcelona, Diagonal 643, Barcelona 08028, Spain

**Running title**: Mycelia enhance bacterial degradation of pollutants

**Keywords:** Pollutant bioavailability; Oomycetes; Biodegradation; Hydrocarbon-degrading bacteria; Polycyclic aromatic hydrocarbons; Non-aqueous phase liquid; Bioremediation

**ABSTRACT:** This work examines the role of mycelia in enhancing the degradation by attached bacteria of organic pollutants that have poor bioavailability. Two oomycetes, *Pythium oligandrum* and *Pythium aphanidermatum*, were selected as producers of mycelial networks, while *Mycobacterium gilvum* VM552 served as a model polycyclic aromatic hydrocarbon (PAH)-degrading bacterium. The experiments consisted of bacterial cultures exposed to a non-disturbed non-aqueous phase liquid (NAPL) layer containing a heavy fuel spiked with $^{14}$C-labeled phenanthrene that were incubated in the presence or absence of the mycelia of the oomycetes in both shaking and static conditions. At the end of the incubation, the changes in the total alkane and PAH contents in the NAPL residue were quantified. The results revealed that with shaking and the absence of mycelia, the strain VM552 grew by utilizing the bulk of alkanes and PAHs in the fuel; however, biofilm formation was incipient and phenanthrene was mineralized following zero-order kinetics, due to bioavailability limitation. The addition of mycelia favored biofilm formation and dramatically enhanced the mineralization of phenanthrene, up to 30 times greater than the rate without mycelia, possibly by providing a physical support to bacterial colonization and by supplying nutrients at the NAPL/water interface. The results in the static condition were very different because the bacterial strain alone degraded phenanthrene with sigmoidal kinetics but could not degrade alkanes or the bulk of PAHs. We suggest that bacteria/oomycete interactions should be considered not only in the design of new inoculants in bioremediation, but also in biodegradation assessments of chemicals present in natural environments.

## GRAPHICAL ABSTRACT

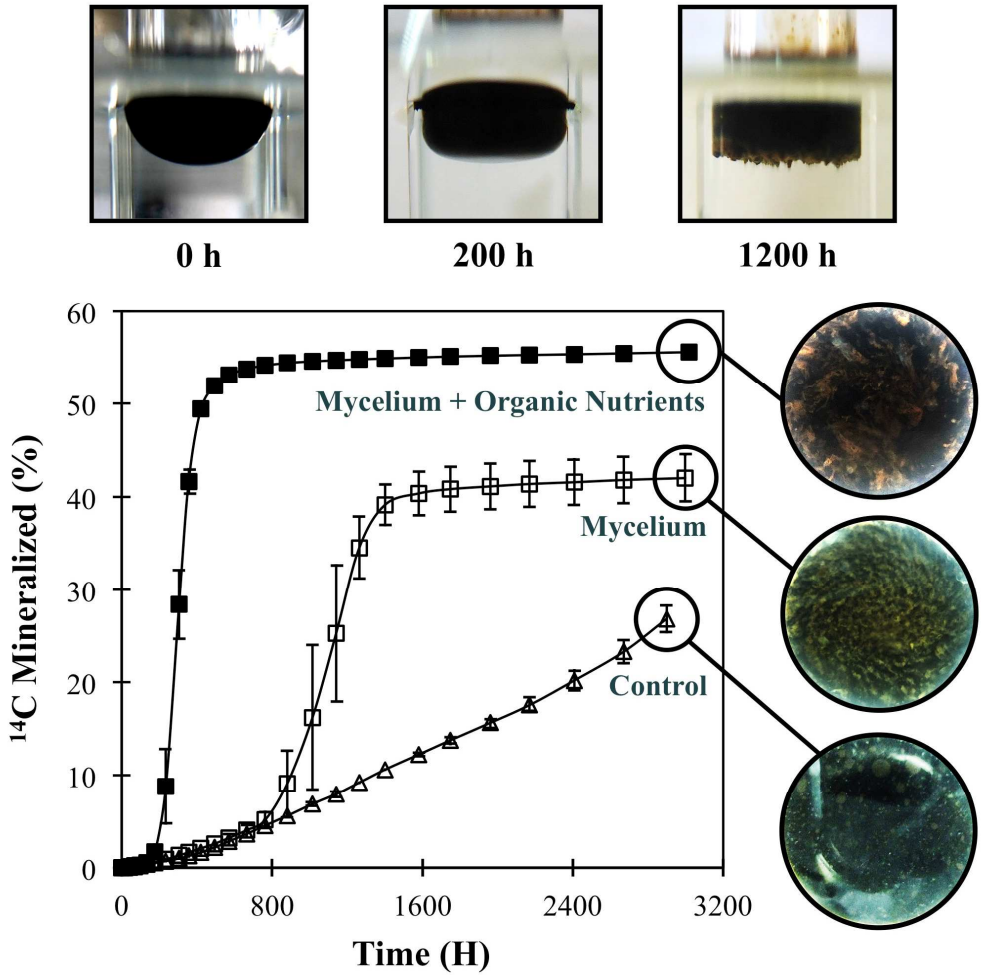

## INTRODUCTION

Hydrophobic organic pollutants (e.g., polycyclic aromatic hydrocarbons (PAHs)), due to their low aqueous concentrations, often exhibit low bioavailability, which limits the metabolic activities and affects the community structures of pollutant-degrading microorganisms.[1-8] Examples of chemicals with restricted bioavailability include PAHs sorbed to natural organic matter and associated with non-aqueous phase liquids (NAPLs), e.g., crude oil and lubricants, matrices in which these chemicals show a reduced chemical activity.[4-7] Recent attempts to enhance the bioavailability and biodegradation of PAHs provided new insights into low-risk ecological approaches to optimizing bioremediation.[6] One approach is the exploitation of natural chemical enhancers (e.g., biosurfactants and plant root exudates) to accelerate the partitioning rate of PAHs from NAPLs or boost the tactic responses of PAH-degrading bacteria toward distant pollutant sources.[2-4,7-9] Additionally, improvements in pollutant bioavailability using mycelial networks formed by eukaryotic microbes (e.g., fungi and oomycetes) have recently been proposed as promising biological enhancers for facilitating the transport of PAH-degrading bacteria and PAHs, leading to increased rates of biodegradation.[10-13]

Two conceptual applications of mycelial networks are considered in the bioremediation of PAH-polluted scenarios.[10-15] First, the mycelial networks provide thin liquid films of water as routes that induce self-propelled PAH-degrading bacteria to perform tactic responses toward PAHs. Second, the extended hyphae within the growing mycelial networks provide linked cytoplasmic channels as the routes for pollutant transport. Although increasing PAH bioavailability is an established role of mycelial networks in ecologically adapted bioremediation, the optimum application of mycelial networks remains uncertain. For example, how can mycelial networks promote

the transport and metabolic activities of non-propelled PAH-degrading bacteria? Hence, the examination of the dynamics of PAHs in low bioavailability scenarios and the presence of mycelia would demonstrate what functions and mechanisms by which mycelia could perform and impact metabolic activities of PAH-degrading bacteria.

Recently, our studies revealed that the motile offspring, so-called "zoospores," produced from mycelial networks of the oomycete *Pythium aphanidermatum* mobilized both non- and self-propelled PAH-degrading bacteria and formed microbial consortia at NAPL/water interfaces.[16,17] Such microbial consortia are initiated by the settlement of zoospores at the interfaces between NAPLs and water, which is followed by germination and the formation of mycelial networks by zoospore cysts onto and into the NAPLs. This sequential phenomenon is likely the initiation of complex biofilms that can enhance PAH bioavailability and sustain the growth of PAH-degrading bacteria.[18-20] However, the structures and roles of biofilms formed at the NAPL/water interface remain poorly known, particularly those of PAH-degrading bacteria and mycelial networks. Further evaluations of the interactive links between these biofilms and the biodegradation of restricted bioavailable PAHs could therefore provide an optimal implementation of such microbial consortia in bioremediation.

With the aim of elucidating the ecological applications of mycelial networks in the bioremediation of low-bioavailable pollutants, we established a model pollution scenario in which PAHs were in a biphasic NAPL/water system prepared with a heavy fuel oil/alkane mixture. The system allows a low chemical activity of the PAHs due to their association to the NAPL, thus restricting their bioavailability, and it maintains the integrity of the organic phase and hence a constant interfacial area.[7] The bacterium *Mycobacterium gilvum* VM552 was selected as a non-propelled pollutant-degrader, and two oomycetes, *Pythium oligandrum* and *P. aphanidermatum*, were used as the

producers of mycelial networks. The experiments were constructed in a biometer system under shaken and static conditions, and the dynamics of phenanthrene as a model PAH was tracked with isotope labeling. At the end of the incubation, the changes in the total alkane and PAH contents in the NAPL residue were quantified. The links between the interfacial biofilms of the microbial co-cultures and the PAH-degrading activities of the bacterium are discussed in this study.

## MATERIALS AND METHODS

**Chemicals.** PAHs, phenanthrene-9-$^{14}$C (13.1 mCi mmol$^{-1}$, radiochemical purity > 98%), 2,2,4,4,6,8,8-heptamethylnonane (HMN), and 17$\alpha$(H),21$\beta$(H)-hopane were purchased from Sigma-Aldrich, Germany. Heavy fuel oil RMG 35 (ISO 8217) was obtained from the Technical Office of Accidental Marine Spills, University of Vigo, Spain.[7]

**Microbial Strains, Cultivation and Preparation.** *M. gilvum* VM552 (a PAH-degrading bacterium) was supplied by D. Springael (Catholic University of Leuven, Belgium). This bacterium can utilize various PAHs and alkanes as carbon and energy sources. The bacterial strain was preserved in 20% (v/v) glycerol at –80°C. The bacterium was grown on tryptic soy agar (Sigma-Aldrich, Germany) at 30°C for 4 – 7 days and then transferred to a mineral salt medium supplemented with 0.02 g mL$^{-1}$ of phenanthrene as the sole source of carbon and energy.[7] The inoculated culture broth was incubated at 30°C with shaking at 150 rpm. When the culture reached the exponential phase of growth (~96 h of incubation), the excess phenanthrene was removed by filtration through a glass fiber filter (pore size, Ø = 40 μm). The culture filtrate was then incubated overnight under the same growing conditions described above for complete phenanthrene removal by biodegradation. Bacterial cells were collected by

centrifugation at 4303 ×*g*, washed twice, and re-suspended in sterilized lake water (by autoclaving at 121°C for 15 min). This natural lake water was collected at Embalse Torre del Águila, Seville, Spain, and kept frozen (-80°C) until use. The lake water is an optimal solution for oomycete development and has a low concentration of dissolved organic carbon (9 mg $L^{-1}$), as well as traces of phosphorus (P) and nitrogen (N).[16] Bacterial cell density was adjusted at 600 nm absorbance ($OD_{600\ nm}$) to 1 (corresponding to ~$10^8$ colony forming units or CFU $mL^{-1}$), which was used further as an inoculum for mineralization experiments.

Two oomycetes, *P. oligandrum* and *P. aphanidermatum*, were used in this study. *P. oligandrum* CBS 530.74 (a mycoparasitic oomycete used as a biocontrol agent against pathogenic fungi and oomycetes) was purchased from Centraalbureau voor Schimmelcultures (CBS), Fungal Biodiversity Centre, Institute of the Royal Netherlands Academy of Arts and Sciences, Utrecht, The Netherlands. *P. aphanidermatum* (a massive zoospore-producing oomycete) was supplied by the Aberdeen Oomycete Laboratory, University of Aberdeen, UK. Both oomycetes are able to form mycelia (filamentous growth) on solid agar medium and to produce biflagellate zoospores under certain conditions (e.g., submerged and aqueous environments). However, we did not observe zoospores produced by *P. oligandrum* under the same conditions used for zoospore formation of *P. aphanidermatum*. The two oomycetes were grown routinely on diluted V8 (DV8) agar medium following the protocol described elsewhere.[16] DV8 agar medium contains V8 juice (Campbell Soup Company, UK). According to the analysis of a sample performed in our laboratory, this medium has 548 mg $L^{-1}$ of total organic carbon, 820 mg $L^{-1}$ of total N and 157 mg $L^{-1}$ of total P. Although both oomycetes form mycelia on this agar medium, the density of biomass (mycelia) per area of growth (μg $cm^{-2}$) was different. *P. aphanidermatum* could form 2-

time denser mycelia than *P. oligandrum* (data not shown). Two different forms of mycelia were prepared as the inocula for the mineralization experiments, including solely mycelia (no DV8 agar medium) and mycelia growing on DV8 agar medium (mycelia + DV8). After growing each oomycete on DV8 agar medium for 4 days, the seeded agar medium was cut into pieces of 1 $cm^2$. The inoculum with solely mycelia was prepared after removing DV8 agar medium by scraping aerial mycelia from the medium surfaces, while mycelia-growing agar pieces served as the inoculum of mycelia + DV8. A total of 20 pieces of either mycelia or mycelia + DV8 was introduced in an individual mineralization assay.

**Mineralization Experiments and Rate Determination.** The experiments were performed using a biometer flask that contained a trap (1 mL of 0.5 M NaOH) for $CO_2$ and an open-end glass cylinder (Ø = 2 cm, 10 cm length, and four 2-mm slots in the base) to maintain the physical integrity of the NAPL/water interface, as described elsewhere.[7] Sterilized lake water (70 mL) was introduced into the flask and mixed with 1 mL of bacterial suspension to give a final concentration of approximately $10^7$ CFU $mL^{-1}$. The flask was then supplemented with 1) 20 pieces of oomycete mycelia (solely mycelia), 2) 20 pieces of mycelia-growing DV8 agar medium (mycelia + DV8), or 3) 20 pieces of DV8 agar medium (solely DV8). The control flasks had only the bacterial suspension or only the mycelia-growing DV8 agar medium of each oomycete (20 pieces in total as well). Within the prepared biometer flasks, 1 mL of NAPL was added to the open-end glass cylinder fixed at the center of the flask. The NAPL was a mixture of heavy fuel oil with HMN at a 1:1 ratio (w/v) to reduce the fuel viscosity. The radiolabeled $^{14}$C-phenanthrene was added to the NAPL at an approximate final concentration of 50,000 dpm $mL^{-1}$, and the solution was homogenized by shaking at

150 rpm for a few hours. The cylinder base allowed the circulation of the medium from outside, and prevented the contact of the agar pieces with the NAPL/water interface.

The mineralization experiments were performed at least in duplicate and incubated at 25°C either aerated by shaking reciprocally at 80 rpm or in a static condition. One mL of NaOH added in the biometer flasks was continuously collected and replaced with new one along the mineralization experiments till the mineralization curves reached the aged plateau phases (approximately 125 days for shaken conditions and up to 190 days for static conditions). The $^{14}CO_2$-trapped NaOH was measured for its radioactivity after mixed with scintillation cocktail by using an LS 6500 Scintillation Counter (BECKMAN COULTER, USA). The mineralization activity of *M. gilvum* VM552 was estimated by the production of $^{14}CO_2$. No significant loss of $^{14}CO_2$ was expected during the mineralization experiments because all biometer flasks were sealed with Teflon-lined closures. This closed biometer flask system was verified for $^{14}CO_2$ losess in previous work with soils and showed the complete recovery of non-mineralized $^{14}C$ residues by combustion of the solids in a biological oxidizer.[21] The mineralization rate of phenanthrene by strain VM552 was calculated using at least five successive points derived from the mineralization curve of the $^{14}C$ mineralized versus incubation time. The 5 successive points were selected from the slope of each mineralization curve, approximately at mid-log phase for the sigmoid curve and approximately at mid-phase for the straight-line curve. The initial mass of phenanthrene in 1 mL of NAPL was 210 μg; one dpm of $^{14}C$-labeled phenanthrene corresponded to 4.2 ng of the total phenanthrene.

**End-Point Mass Balance of $^{14}C$ and Characterization of NAPL Residues.** At the end of the mineralization experiments, the NAPL residues were gently removed from biometer flasks, and all the remaining solids were separated from the aqueous

phase by centrifugation at 4303 ×*g* for 10 min. The solids were re-suspended in a known volume of distilled water and dispersed roughly with a spatula. The suspension was then sonicated for 1 h in a sonicator bath (Branson 3510) and homogenized with a vortex for a few min. The radioactivity in the solid and the aqueous phase was determined with the scintillation counter. The percentage of $^{14}C$ remaining in the NAPL was calculated by the difference between the total $^{14}C$ recovered and the initial $^{14}C$. The direct measurement of this fraction was not possible because of inflammability and quenching caused by the fuel present in the samples.

The collected NAPL residues were subsequently analyzed for their hydrocarbon composition. Each NAPL sample was dissolved in dichloromethane, dried over $Na_2SO_4$ and concentrated to 5 mL. The saturated and aromatic hydrocarbon fractions were then separated by column chromatography following US-EPA method 3611b and analyzed by GC-MS as described elsewhere.[22] The degradation percentages of the fuel total alkanes and of US-EPA PAHs and alkyl derivatives were determined by comparing the hopane-normalized areas from reconstructed ion chromatograms to those obtained from controls. The alkanes were determined using *m/z* 85 as a diagnostic ion, while PAHs and their alkyl derivatives were detected using their corresponding molecular ions.[23] 17$\alpha$(H),21$\beta$(H)-hopane was used as the conserved internal marker (ion *m*/*z* 191). The alkane HMN was not analyzed because it was used as a non-degradable component of the NAPL.[7,16]

To evaluate the effect of biofilms formed at the NAPL/water interfaces on the mineralization activities of *M. gilvum* VM552, we observed the macroscopic changes in biofilm growth and NAPL hydrophobicity during the mineralization experiments. The NAPL/water interfaces were screened for biofilm growth by direct observation, and the detected biofilms were photographed at the end of the mineralization experiments. The

248 microscopic structures of the interfacial biofilms were also photographed after staining
249 with 0.02% (v/v) acridine orange and visualizing with a fluorescence microscope
250 (Axioskop 2 Carl Zeiss, Jena, Germany). The NAPL hydrophobicity was determined by
251 measuring the contact angle ($\theta_{nw}$) after perpendicular photography of the buoyant
252 NAPL fixed in the glass cylinder at the center of each biometer flask. With the aim of
253 discriminating the impacts of growth and development of oomycetes on the levels of
254 dissolved oxygen (DO) and dissolved organic carbon (DOC) that would cause some
255 influence on the bacterial degradation, we also measured these parameters. A set of
256 experiments imitating the mineralization experiments was carried out, using an oxygen
257 meter (OXI 45 DL, CRISON) for DO and a Shimadzu TOC-VCSH with ASI-V auto
258 sampler after filtration through Whatman® No. 1 (pore size, Ø = 11 μm) for DOC.

259 **Statistical Analyses.** The mean value ± standard deviation (SD) or standard error
260 (SE) derived from any measurement is reported. Comparison of multiple means was
261 performed by appropriate analysis of variance (ANOVA) with Tukey's *post hoc* test in
262 the SPSS 21.0 program (SPSS, Chicago, IL, USA). The statistical results are reported
263 with the *F*-distribution, degrees of freedom and significant (*P*) value.

264

265 **RESULTS AND DISCUSSION**

266 **Enhancement of Pollutant Biodegradation by Mycelia.** The effects of *P.*
267 *oligandrum* and *P. aphanidermatum* mycelia on the bacterial mineralization of
268 phenanthrene initially present in the NAPL are shown in Figure 1 and Supporting
269 Information (SI) Figure S1, respectively. Under shaking conditions (Figure 1a), *M.*
270 *gilvum* VM552 mineralized phenanthrene at a slow rate and following zero-order
271 kinetics. The mineralization curves in the presence of *M. gilvum* VM552 and the
272 oomycetes were S shaped (logistic kinetics). When the oomycetes growing on DV8 agar

were supplied, the bacterial metabolism occurred at significantly higher rates than in the presence of the bacterium only (Table 1). *P. oligandrum* caused a greater enhancement of the bacterial mineralization of phenanthrene than *P. aphanidermatum*. Such difference in the enhancement caused by distinct oomycete species suggested that the effect was highly dependent upon the growth and development of oomycetes. The control supplemented with DV8 agar alone showed a stimulatory effect on *M. gilvum* VM552, but the maximum mineralization rates were significantly higher when the oomycetes were also present. The other controls containing only the oomycetes growing on DV8 agar resulted in negligible rates of mineralization of phenanthrene (lower than 0.01 ng $mL^{-1}$ $h^{-1}$), which confirmed that the bacterium was solely responsible for the transformation.

In our previous work, static conditions were identified as favorable for oomycete growth and development in a set of PAH-polluted scenarios.[16,17] Therefore, we conducted a set of mineralization experiments in which the flasks were allowed to stand without further shaking. The static conditions resulted in two contrasting effects on phenanthrene mineralization. First, *M. gilvum* VM552 alone mineralized phenanthrene following logistic kinetics (Figure 1b) with a maximum rate that was significantly higher than the rate under shaking conditions (Table 1). Second, the static conditions led to a significantly lower rate of phenanthrene mineralization in the treatment with *M. gilvum* VM552 and the oomycetes growing on DV8 agar than the shaking conditions (Table 1). However, the rate remained significantly higher than the static controls with the bacterium only, with and without DV8 agar. Thus, under static conditions, the mycelia enhanced the transformation.

The relatively high extents of phenanthrene mineralization observed (Table 1) were consistent with the nearly complete consumption of the chemical initially present

298 in the NAPL as demonstrated by GC-MS analysis of the phenanthrene remaining in the
299 NAPL at the end of incubation (Table 2). The analysis showed that the losses of
300 phenanthrene were higher than 95% in all treatments except for the shaken cultures
301 containing only the bacterium. The differences in the extent of mineralization between
302 these treatments (Table 1) could be explained by the incorporation of different
303 proportions of substrate carbon into microbial biomass or transformed to partially
304 oxidized byproducts, which is a characteristic of growth-linked biodegradation.[21]
305 Therefore, the distribution of the non-mineralized phenanthrene carbon was determined
306 (Table 2). Despite the nearly complete phenanthrene disappearance, the results
307 indicated that a significantly high percentage of $^{14}C$ remained associated with the NAPL
308 at the end of incubation (up to 35.21% in the treatment with *P. oligandrum* mycelia
309 under shaken conditions, Table 2). Very low percentages of $^{14}C$ (0.32 – 2.42%) were
310 detected in the aqueous and solid fractions of the treatments that contained the
311 oomycete growing on DV8 agar (Table 2). These findings are consistent with the
312 negligible metabolism of phenanthrene by the oomycete, as well as the low sorption of
313 the chemical to the oomycete biomass.

314 The strain *M. gilvum* VM552 was selected for this study because of its capacity to
315 mineralize phenanthrene, but this bacterium can also degrade other PAHs and alkyl
316 derivatives in addition to alkanes present in the fuel. The degradation pattern by *M.*
317 *gilvum* VM552 of the different components of this fuel mixture is described elsewhere.[7]
318 In this study, the GC-MS analysis of the NAPL residues at the end of incubation
319 showed the biodegradation of the primary components in the NAPL, including both
320 aromatic and aliphatic hydrocarbons, under shaking conditions (SI Table S1 and Figures
321 S2 and S3). The treatment containing only *P. oligandrum* exhibited the typical profile
322 of the non-degraded fuel and was therefore chosen as the reference for the other

treatments.[7] Co-inoculation with the oomycete mycelia and the addition of DV8 had no effect on the final extent of the biodegradation of total PAHs and alkanes under shaking conditions. However, very limited bacterial degradation of the bulk of the fuel components was observed under static conditions (SI Table S1). The selective degradation of phenanthrene (Table 2) was consistent with the fact that the strain had been pre-grown with this substrate as the sole carbon source (the phenanthrene-degrading enzymes were present) and its very low concentration compared with that of the other individual fuel components (4.3% of total PAHs).

**Roles of Mycelia in Promoting Bacterial Colonization at the NAPL/Water Interface.** The NAPL in contact with the microbial suspension formed a stable interface between this hydrophobic layer and the water, where the phase exchange of chemicals took place. Our results in Tables 1 and 2 indicated that the mycelia enhanced the biodegradation of phenanthrene through the stimulation of microbial colonization of the NAPL/water interface. In the absence of mycelia and under shaking conditions, the mineralization of phenanthrene occurred linearly at a constant rate that was very similar to the partitioning rate of the chemical (0.2 ng $mL^{-1}$ $h^{-1}$) measured under the same conditions (i.e., NAPL/water interface area and shaking speed) in a previous study from our group, what indicates bioavailability restrictions.[7] However, mycelia enhanced the mineralization rates of phenanthrene by the bacterium, which exceeded those of the partitioning rate predictions (Table 1). Logistic, partitioning uncoupled kinetics can be observed during the biodegradation of organic chemicals in NAPLs, when the microorganisms proliferate attached to the NAPL/water interfaces, where they acquire directly the chemicals.[4,7,24] The significant presence of non-mineralized phenanthrene C in the NAPL at the end of the experimental period, when phenanthrene had disappeared

347 (Table 2), could be attributed to the attached bacterial cells that had assimilated the
348 chemical.

349 The morphology of the NAPL/water interface was observed during the
350 mineralization experiments to determine if physical changes at the NAPL/water
351 interface, induced by the mycelia, were linked to bacterial degradation. In side view, the
352 NAPL displayed a convex shape at the start of the experiments, which gradually
353 changed during the incubation (Figure 2a). The changes in the NAPL side views
354 corresponded to the evolution of the NAPL/water contact angle ($\theta_{nw}$), which was
355 associated to the NAPL hydrophobicity. The $\theta_{nw}$ value was approximately 120° at the
356 start of the experiments and gradually decreased during the experimental period. Such
357 macroscopic changes were attributed to a reduction of the NAPL hydrophobicity, which
358 were observed in most treatments regardless the different conditions tested and were
359 associated with the kinetics of phenanthrene mineralization (Table 1 and Figure 1).
360 Under shaking conditions, the change of the NAPL/water contact angle was more rapid
361 when mycelia were present, which was consistent with the onset in the mineralization
362 rates (Figure 1a). The unchanged $\theta_{nw}$ value of the controls without the bacterium
363 corresponded with the negligible biodegradation of the NAPL components (including
364 phenanthrene) in addition to the absence of apparent growth of the oomycetes (Table 1).
365 These findings indicated that in addition to wettability and contact time,[25,26] microbial
366 communities dwelling at the NAPL/water interface also have a significant effect on the
367 NAPL hydrophobicity.

368 The interfacial biofilms were macroscopically observed at the end of the
369 mineralization experiments, and the biofilms were relatively denser in the treatments
370 with oomycete mycelia (Figure 2b). Such abundant biofilms were relevant to the
371 apparent macroscopic changes of the fuel layer, as reflected by the evolution of the $\theta_{nw}$.

The aspect of the biofilms was also different depending upon the treatment. For example, in shaking conditions, the pattern of colonization in the treatment with only *M. gilvum* VM552 cells was characterized by discrete colonies randomly formed throughout the fuel surface, while in those treatments with mycelial supplements, a swirl pattern developed as a result of reciprocal shaking (Figure 2b). We confirmed by epifluorescence microscopy, the presence of both microbial components (*M. gilvum* VM552 cells and oomycete mycelium) in the biofilms formed at the NAPL/water interfaces.

The mechanism by which oomycetes facilitated biofilm formation at the NAPL/water interface could be based on a biophysical effect. The colonization of the interface by mycelia possibly occurred through the filamentous growth and/or the release of reproductive propagules (e.g., hyphal fragments, oospores and zoospores), what formed mycelial networks at the interface.[12,16,24] Such networks can provide paths for bacterial transport to reach and colonize the NAPL/water interface, which is a well-known mechanism, called the "fungal highway effect", for enhancing pollutant bioavailability and biodegradation.[11-15] This biophysical facilitation was observed with the hydrophilic mycelia of *Pythium ultimum*,[13] which belongs to the same phylogenetic cluster of both oomycete species used in this work. Also, *Mycobacterium* spp. can perform surface motility on moist or wet surfaces, although their cells are hydrophobic and non-flagellated.[12,27] The floating mycelia might play some role in moderating the Brownian motion of bacterial cells by reducing the shear forces within the aqueous microenvironments caused by shaking. It is also possible that oomycetes release zoospores that have a tactic response to diverse substrata (including pollutant/water interfaces) at the remote microhabitats in which they settle and initiate sibling mycelial networks.[16,17,28] Indeed, oomycete zoospores are able to mobilize directionally *M.*

397 *gilvum* VM552 cells under a steady-flow environment.[17] Moreover, *P. aphanidermatum*
398 zoospores exhibited selective settlement and formed hyphae penetrating a single-
399 component NAPL (hexadecane),[16] which is relevant to this study as hexadecane is also
400 an alkane component of heavy fuel oil (SI Figure S2).

401 It is also possible that the growth and development of the oomycetes at the
402 NAPL/water interface provided an exchange platform for essential metabolites and
403 elements. In this context, the logistic kinetics observed with DV8 medium was
404 consistent with this nutritional effect at the NAPL/water interface. The selective
405 biodegradation of phenanthrene under static conditions that occurred in the absence of
406 mycelia and DV8 medium can also be understood because under these conditions, the
407 diffusion of oxygen also limited bacterial metabolism and biosynthesis at the interface.
408 The higher percentages of phenanthrene degradation than those of the bulk of the PAHs
409 corresponded to the relatively low concentration of phenanthrene in the fuel and the
410 preference of the strain for this substrate under such conditions. In fact, the inoculated
411 *M. gilvum* VM552 cells were pre-grown on phenanthrene and could readily and
412 selectively mineralize this compound. According to this mechanism, attached bacteria
413 mineralized phenanthrene under static conditions at an even higher rate than under
414 shaking conditions (i.e. even when partitioning of the chemical was expected to be
415 slower, relying on diffusion only), because the simultaneous consumption of the other
416 NAPL components, with the subsequent competition effects, did not occur. This made
417 the stimulation by the oomycetes (and the DV8 medium) less evident. Alternately, it is
418 also possible that, under static conditions, more *M. gilvum* VM552 cells could have
419 accumulated at the interface, resulting in a faster phenanthrene mineralization. However,
420 this explanation is unlikely because it is not consistent with the preferential

421 phenanthrene biodegradation observed in static conditions (i.e. the other NAPL
422 components were not degraded at a higher extent).

423 **Roles of dissolved oxygen and dissolved organic carbon.** Because the growth
424 and development of oomycetes could modify the concentration of dissolved oxygen
425 (DO), which would have an effect on the biodegradation of hydrocarbons (particularly
426 under static conditions), the concentrations of DO were measured. The measurements
427 were performed in the absence of NAPL and bacterial inoculum, to prevent any
428 interference from, respectively, NAPL toxicity and bacterial consumption of DO, but
429 the rest of the conditions were kept the same as for the mineralization experiments (SI
430 Figure S4). The DO levels always remained at approximately 6 mg $L^{-1}$ during the
431 experimental period of 700 h, regardless of whether the biometer flasks were inoculated
432 with the oomycetes or incubated under shaking or static conditions. The growth of
433 oomycetes was also confirmed macroscopically at the end of the assay. The levels of
434 DO revealed the concentration of DO was not limiting for bacterial degradation. The
435 concentrations of DO detected in this study are much higher than the half-saturation
436 coefficient for DO ($K_{DO}$ = 0.094 mg $L^{-1}$) that *Mycobacterium* requires to reach the
437 maximum growth rate in the presence of a single PAH.[29] Also, a DO concentration as
438 low as 0.034 mg $L^{-1}$ has no influence on alkane biodegradation in sediment
439 microcosms.[29]

440 A possible role of mycelia in the production of dissolved organic carbon (DOC),
441 which could have enhanced the biodegradation of hydrocarbons by increasing their
442 partitioning rates from the NAPL to the aqueous phase, driven by sorption to dissolved
443 macromolecules, [8,30] was also examined. The concentration of DOC was determined in
444 assays that simulated the conditions during the mineralization experiments but without
445 the NAPL and the bacterium (SI Figure S5). Without any oomycete inoculum and under

446 both shaking and static conditions, the DV8 agar blocks passively released DOC to
447 reach an equilibrium concentration of 150 mg $L^{-1}$ after 480 h of the incubation. The
448 equilibrium concentration of DOC was significantly lower when the assays were
449 inoculated with the oomycete growing on DV8 agar (100 mg $L^{-1}$) and with the
450 oomycete mycelia only (20 mg $L^{-1}$). No significant effect was detected between the
451 shaking and static conditions on the variation of DOC concentration. In theory, these
452 low DOC concentrations were not sufficient to cause an enhancement in the net
453 partitioning of phenanthrene into the aqueous phase, which would explain the
454 mineralization rates in this study. Taking into account a DOC concentration of 150 mg
455 $L^{-1}$ in the aqueous phase and the log $K_{oc}$ of phenanthrene, which is 4.16,[16] the predicted
456 total concentration of the compound in the aqueous phase (and the resulting net
457 partitioning rate, assuming instantaneous equilibrium with DOC)[8,30] was only enhanced
458 by 3-fold, which is significantly lower than the 10-fold enhancement observed (Table 1).
459 However, assuming a general figure of 1 pg C/microbial cell,[21] the complete
460 transformation into bacterial cells of the DOC released from the DV8 agar would have
461 caused a 15-fold increase of the bacterial population initially present ($10^7$ cells/mL). It
462 is possible, therefore, that the DV8 agar contributed to increase the density of suspended
463 bacteria, which eventually attached to the NAPL/water interface, thus promoting its
464 colonization.

465 In summary, the data show that mycelia enhanced the bacterial degradation of
466 hydrophobic organic pollutants under the bioavailability restrictions imposed by a
467 NAPL. Promoting bacterial colonization at the pollutant/water interfaces through a
468 biophysical effect, by facilitating the translocation of bacteria through the radial
469 expansion of mycelial growth and release of productive propagules, and providing an
470 exchange platform for metabolites and minerals at the interface, are proposed here as

471 the possible mechanisms for the enhancement of pollutant bioavailability and
472 biodegradation. The exact mechanisms operating under static conditions, that may be
473 representative of some environments, such as soil, will be the subject for further
474 research. Nevertheless, this study provides new insights into the role of
475 bacteria/oomycete interactions in the colonization of interfaces, which is important for
476 designing new inoculants in bioremediation. The results have also implications for
477 studies focused on the persistence of chemicals in natural environments, by highlighting
478 the possible influence of mycelia on the activity of pollutant-degrading bacterial
479 communities that develop at the surfaces of NAPLs and aggregates in soils and
480 sediments.
481

482 **ASSOCIATED CONTENT**

483 **Supporting Information**

484 (Table S1) Effect of *Pythium oligandrum* on bacterial degradation (%) of total PAHs
485 and alkanes initially present in the non-aqueous phase liquid; (Figure S1) Effect of
486 *Pythium aphanidermatum* mycelium on bacterial mineralization of $^{14}$C-phenanthrene
487 initially associated with the NAPL; (Figure S2) Effect of *Pythium oligandrum* on the
488 hopane-normalized areas ($A/A_{Hop}$) of PAHs and alkyl-PAHs analyzed by molecular
489 ions based GC-MS; (Figure S3) Effect of *Pythium oligandrum* on the hopane-
490 normalized areas ($A/A_{Hop}$) of *n*-alkanes analyzed by *m*/*z* 85-based GC-MS; (Figure S4)
491 Evolution of dissolved oxygen (DO) concentration in the aqueous phase of
492 mineralization experiments; (Figure S5) Evolution of dissolved organic carbon (DOC)
493 concentration in the aqueous phase of mineralization experiments.
494

495 **AUTHOR INFORMATION**

**Corresponding Author**

*Phone: (+34) 954 624 711; Fax: (+34) 954 624 002;

E-mail: jjortega@irnase.csic.es.

**Present Address**

‖Infrastructure and Environmental Research Division, School of Engineering, University of Glasgow, Glasgow G12 8LT, UK.

**Notes**

The authors declare no competing financial interest.

**ACKNOWLEDGMENTS**

We thank the Spanish Ministry of Science and Innovation (CGL2010-22068-C02-01, CGL2013-44554-R and CGL2016-77497-R), the Andalusian Government (RNM 2337), the European Commission (LIFE15 ENV/IT/000396) and the CSIC JAE Program (RS) for funding support.

**REFERENCES**

(1) Chen, B.; Wang, Y.; Hu, D. Biosorption and biodegradation of polycyclic aromatic hydrocarbons in aqueous solutions by a consortium of white-rot fungi. *J. Hazard. Mat.* **2010**, *179*, 845–851.

(2) Zhu, H.; Aitken, M. D. Surfactant-enhanced desorption and biodegradation of polycyclic aromatic hydrocarbons in contaminated soil. *Environ. Sci. Technol.* **2010,** *44*, 7260-7265.

(3) Thompson, I. P.; van der Gast, C. J.; Ciric, L.; Singer, A. C. Bioaugmentation for bioremediation: the challenge of strain selection. *Environ. Microbiol.* **2005,** *7*, 909-915.

(4) García-Junco, M.; De Olmedo, E.; Ortega-Calvo, J. J. Bioavailability of solid and non-aqueous phase liquid (NAPL)-dissolved phenanthrene to the biosurfactant-producing bacterium *Pseudomonas aeruginosa* 19SJ. *Environ*. *Microbiol*. **2001**, *3*, 561–569.

(5) Krell, T.; Lacal, J. S.; Reyes-Darias, J. A.; Jimenez-Sanchez, C.; Sungthong, R.; Ortega-Calvo, J. J. Bioavailability of pollutants and chemotaxis. *Curr*. *Opin*. *Biotechnol*. **2013**, *24*, 451–456.

(6) Ortega-Calvo, J. J.; Tejeda-Agredano, M. C.; Jimenez-Sanchez, C.; Congiu, E.; Sungthong, R.; Niqui-Arroyo, J. L.; Cantos, M. Is it possible to increase bioavailability but not environmental risk of PAHs in bioremediation? *J*. *Hazard*. *Mat*. **2013**, *261*, 733–745.

(7) Tejeda-Agredano, M. C.; Gallego, S.; Niqui-Arroyo, J. L.; Vila, J.; Grifoll, M.; Ortega-Calvo, J. J. Effect of interface fertilization on biodegradation of polycyclic aromatic hydrocarbons present in nonaqueous-phase liquids. *Environ*. *Sci*. *Technol*. **2011**, *45*, 1074–1081.

(8) Tejeda-Agredano, M. C.; Mayer, P.; Ortega-Calvo, J. J. The effect of humic acids on biodegradation of polycyclic aromatic hydrocarbons depends on the exposure regime. *Environ*. *Pollut*. **2014**, *184*, 435–442.

(9) Jimenez-Sanchez, C.; Wick, L. Y.; Ortega-Calvo, J. J. Chemical effectors cause different motile behavior and deposition of bacteria in porous media. *Environ*. *Sci*. *Technol*. **2012**, *46*, 6790–6797.

(10) Furuno, S.; Foss, S.; Wild, E.; Jones, K. C.; Semple, K. T.; Harms, H.; Wick, L. Y. Mycelia promote active transport and spatial dispersion of polycyclic aromatic hydrocarbons. *Environ*. *Sci*. *Technol*. **2012**, *46*, 5463–5470.

(11) Furuno, S.; Päzolt, K.; Rabe, C.; Neu, T. R.; Harms, H.; Wick, L. Y. Fungal mycelia allow chemotactic dispersal of polycyclic aromatic hydrocarbon-degrading bacteria in water-unsaturated systems. *Environ*. *Microbiol*. **2010**, *12*, 1391–1398.

(12) Kohlmeier, S.; Smits, T. H.; Ford, R. M.; Keel, C.; Harms, H.; Wick, L. Y. Taking the fungal highway: mobilization of pollutant-degrading bacteria by fungi. *Environ*. *Sci*. *Technol*. **2005**, *39*, 4640–4646.

(13) Wick, L. Y.; Remer, R.; Würz, B.; Reichenbach, J.; Braun, S.; Schäfer, F.; Harms, H. Effect of fungal hyphae on the access of bacteria to phenanthrene in soil. *Environ*. *Sci*. *Technol*. **2007**, *41*, 500–505.

(14) Banitz, T.; Johst, K.; Wick, L. Y.; Schamfuß, S.; Harms, H.; Frank, K. Highways versus pipelines: contributions of two fungal transport mechanisms to efficient bioremediation. *Environ*. *Microbiol*. *Rep*. **2013**, *5*, 211–218.

(15) Harms, H.; Schlosser, D.; Wick, L. Y. Untapped potential: exploiting fungi in bioremediation of hazardous chemicals. *Nat*. *Rev*. *Microbiol*. **2011**, *9*, 177–192.

(16) Sungthong, R.; van West, P.; Cantos, M.; Ortega-Calvo, J. J. Development of eukaryotic zoospores within polycyclic aromatic hydrocarbon (PAH)-polluted environments: A set of behaviors that are relevant for bioremediation. *Sci*. *Total Environ*. **2015**, *511*, 767–776.

(17) Sungthong, R.; van West, P.; Heyman, F.; Jensen, D. F.; Ortega-Calvo, J. J. Mobilization of pollutant-degrading bacteria by eukaryotic zoospores. *Environ*. *Sci. Technol*. **2016**, *50*, 7633–7640.

(18) Johnsen, A. R.; Karlson, U. Evaluation of bacterial strategies to promote the bioavailability of polycyclic aromatic hydrocarbons. *Appl. Microbiol. Biotechnol.* **2004**, *63*, 452–459.

(19) Seo, Y.; Lee, W. H.; Sorial, G.; Bishop, P. L. The application of a mulch biofilm barrier for surfactant enhanced polycyclic aromatic hydrocarbon bioremediation. *Environ. Pollut.* **2009**, *157*, 95–101.

(20) Mangwani, N.; Kumari, S.; Das, S. Involvement of quorum sensing genes in biofilm development and degradation of polycyclic aromatic hydrocarbons by a marine bacterium *Pseudomonas aeruginosa* N6P6. *Appl. Microbiol. Biotechnol.* **2015**, *99*, 10283–10297.

(21) Niqui-Arroyo, J. L.; Bueno-Montes, M.; Ortega-Calvo, J. J. Biodegradation of anthropogenic organic compounds in natural environments. In *Biophysico-Chemical Processes of Anthropogenic Organic Compounds in Environmental Systems*; Xing, B., Senesi, N., Huang, P. M., Eds.; IUPAC Series on Biophysico-Chemical Processes in Environmental Systems; John Wiley & Sons, Inc.: Hoboken, NJ, **2011**, Vol *3*, 483–501.

(22) Vila, J.; Grifoll, M. Actions of *Mycobacterium* sp. AP1 on the saturated- and aromatic-hydrocarbon fractions of fuel oil in a marine medium. *Appl. Environ. Microbiol.* **2009**, *75*, 6232–6239.

(23) Kostecki, P. T.; Calabrese, E. J. Contaminated soils. In *Diesel fuel contamination*; Lewis Publishers Inc.: Chelsea, Michigan, **1992**.

(24) Harding, M. W.; Marques, L. L.; Howard, R. J.; Olson, M. E. Can filamentous fungi form biofilms? *Trends Microbiol.* **2009**, *17*, 475–480.

(25) Grate, J. W.; Dehoff, K. J.; Warner, M. G.; Pittman, J. W.; Wietsma, T. W.; Zhang, C.; Oostrom, M. Correlation of oil–water and air–water contact angles of

diverse silanized surfaces and relationship to fluid interfacial tensions. *Langmuir* **2012**, *28*, 7182–7188.

(26) Lee, H. B.; Kim, B. W. Effect of NAPL exposure on the wettability and two-phase-flow in a single rock fracture. *Hydrol*. *Process*. **2015**, *29*, 4919–4931.

(27) Fredslund, L.; Sniegowski, K.; Wick, L. Y.; Jacobsen, C. S.; De Mot, R.; Springael, D. Surface motility of polycyclic aromatic hydrocarbon (PAH)-degrading mycobacteria. *Res*. *Microbiol*. **2008**, *159*, 255–262.

(28) Gleason, F. H.; Lilje, O.; Marano, A. V.; Sime-Ngando, T.; Sullivan, B. K.; Kirchmair, M.; Neuhauser, S. Ecological functions of zoosporic hyperparasites. *Front*. *Microbiol*. **2014**, *5*, 244.

(29) Fritzsche, C. Degradation of pyrene at low defined oxygen concentrations by a *Mycobacterium* sp. *Appl*. *Environ*. *Microbiol*. **1994**, *60*, 1687–1689.

(30) Haftka, J. J.; Parsons, J. R.; Govers, H. A.; Ortega-Calvo, J. J. Enhanced kinetics of solid-phase microextraction and biodegradation of polycyclic aromatic hydrocarbons in the presence of dissolved organic matter. *Environ*. *Toxicol*. *Chem*. **2008**, *27*, 1526–1532.

610 **Table 1.** Effect of Oomycete Mycelia on Bacterial Mineralization of $^{14}$C-Phenanthrene Initially Present in the Non-aqueous Phase Liquid[a]

| Treatment | | Maximum mineralization rate (ng mL$^{-1}$ h$^{-1}$) | | Mineralization extent (%) | |
|---|---|---|---|---|---|
| **Inoculum** | **DV8 agar[b]** | **Shaken** | **Static** | **Shaken** | **Static** |
| ***Mycobacterium gilvum* VM552** | - | 0.29 ± 0.04a | 1.31 ± 0.09a* | 26.8 ± 2.0a | 53.2 ± 5.9* |
| | + | 3.24 ± 0.07b | 2.10 ± 0.10b* | 55.5 ± 1.5c | 53.4 ± 0.2 |
| ***M. gilvum* VM552 + *Pythium oligandrum*** | - | 2.03 ± 0.16ab | 1.72 ± 0.22ab | 42.0 ± 4.3b | 51.3 ± 6.7* |
| | + | 8.27 ± 1.21d | 2.90 ± 0.28c* | 55.6 ± 1.3c | 52.2 ± 2.4 |
| ***M. gilvum* VM552 + *Pythium aphanidermatum*** | - | 1.67 ± 0.23ab | 1.75 ± 0.14ab | 28.9 ± 0.2a | 48.9 ± 0.3* |
| | + | 5.86 ± 1.39c | 2.72 ± 0.35c* | 49.6 ± 5.7bc | 53.3 ± 0.7 |

611 [a]The results are reported as the mean ± SD derived from duplicate or triplicate experiments. [b]The treatments contained (+) or did not contain (-) diluted V8 (DV8) agar (see
612 text for details). Values in each column followed by the same lowercase letter are not significantly different according to a one-way ANOVA at $P = 0.05$. Asterisks indicate
613 that the means under static conditions are significantly different from the corresponding values under shaking conditions based on two-way ANOVA and simple main effects
614 tests at $P = 0.05$.

615

616

**Table 2.** Effect of *Pythium oligandrum* Mycelia on Depletion of Phenanthrene Initially Present in the Non-aqueous Phase Liquid (NAPL) and Phase Distribution of Non-mineralized $^{14}C$[a]

| Treatment | | Phenanthrene remaining in NAPL (%)[c] | | Non-mineralized $^{14}C$ (%) | | | | | |
|---|---|---|---|---|---|---|---|---|---|
| | | | | NAPL | | Aqueous | | Solid | |
| Inoculum | DV8 agar[b] | Shaken | Static | Shaken | Static | Shaken | Static | Shaken | Static |
| ***Mycobacterium gilvum* VM552** | - | 28.4 ± 7.4b | 3.19 ± 1.36a* | 53.1 ± 4.3c | 23.0 ± 1.2c* | 14.9 ± 4.2b | 17.9 ± 1.8bc | 4.53 ± 0.04ab | 5.87 ± 2.29b |
| | + | 0.92 ± 0.09a | 2.27 ± 0.49a | 18.8 ± 2.3a | 14.3 ± 2.2ab* | 17.9 ± 2.8b | 18.8 ± 1.8bc | 7.90 ± 2.64bc | 13.4 ± 1.0c* |
| ***M. gilvum* VM552 + *P. oligandrum*** | - | 1.09 ± 0.21a | 2.73 ± 0.05a | 35.2 ± 2.2b | 8.7 ± 4.2a* | 16.5 ± 1.2b | 22.5 ± 2.4c* | 6.27 ± 1.07bc | 17.5 ± 1.8d* |
| | + | 0.89 ± 0.26a | 3.25 ± 0.93a | 16.7 ± 0.6a | 19.6 ± 1.8bc | 17.4 ± 1.3b | 16.9 ± 2.2b | 10.27 ± 0.73c | 11.3 ± 0.8c |
| ***P. oligandrum*** | + | control[d] | control[d] | 96.7 ± 0.5d | 97.9 ± 0.5d | 2.42 ± 0.46a | 1.33 ± 0.22a | 0.50 ± 0.01a | 0.40 ± 0.30a |

[a]The results are reported as the mean percentage ± SD derived from duplicate or triplicate experiments, which were measured at the end of the mineralization experiments. [b]The treatments contained (+) or did not contain (-) diluted V8 (DV8) agar (see text for details). [c]The results are derived from GC-MS analysis. [d]Non-degraded NAPL chosen as the reference for other treatments. Values in each column followed by the same lowercase letter are not significantly different, supported by separate one-way ANOVA at $P = 0.05$. Asterisks indicate that the means under the static condition are significantly different from the corresponding values under the aerated condition based on two-way ANOVA and simple main effects tests at $P = 0.05$.

624 **Figure legends**

625

626 **Figure 1.** Effect of *Pythium oligandrum* mycelia on bacterial mineralization of $^{14}$C-
627 phenanthrene initially associated with the non-aqueous phase liquid (NAPL). The
628 experiments were conducted under shaking (**a**) and static (**b**) conditions. The treatments
629 included *Mycobacterium gilvum* VM552 plus *P. oligandrum* growing on DV8 agar
630 (VM552+PO/DV8), *M. gilvum* VM552 plus *P. oligandrum* mycelia (VM552+PO), *M.*
631 *gilvum* VM552 plus DV8 agar (VM552+DV8), *M. gilvum* VM552 alone as a positive
632 control (VM552), and *P. oligandrum* growing on DV8 agar as a negative control
633 (PO/DV8). Error bars represent the standard error from at least duplicate experiments.

634

635 **Figure 2.** Effects of microbial growth on the morphological evolution of NAPL and
636 macroscopic structures of microbial biofilms colonized at NAPL/water interfaces. The
637 morphological evolution of NAPL determined with the change of contact angle ($\theta_{nw}$)
638 was visualized along the mineralization experiments (a). The macroscopic structures of
639 microbial colonization in form of biofilms at NAPL/water interfaces were photographed
640 at the end of incubation (b). All photographs present in (a) were derived from the
641 experiments under shaken (top) and static (bottom) conditions that contained
642 *Mycobacterium gilvum* VM552 and *Pythium oligandrum* growing on diluted V8 (DV8)
643 agar. The photographs present in (b) refer to all treatments indicated in Figure 1 and SI
644 Figure S1, while the diameters of these photographs correspond to the inner diameters
645 of the glass cylinders (2 cm).

646

647

648

**Figure 1**

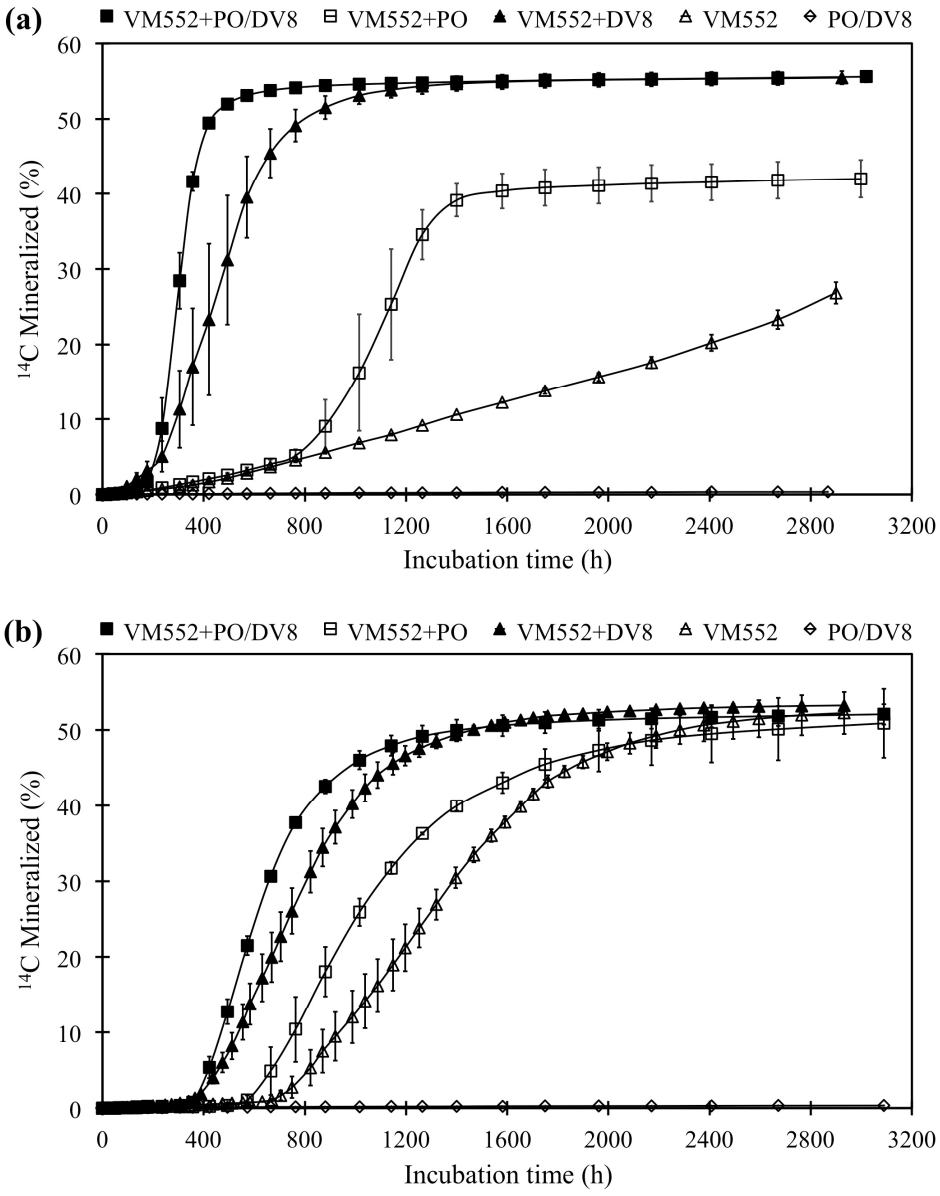
(a)
VM552+PO/DV8
VM552+PO
VM552+DV8
VM552
PO/DV8
$^{14}$C Mineralized (%)
Incubation time (h)
(b)
VM552+PO/DV8
VM552+PO
VM552+DV8
VM552
PO/DV8
$^{14}$C Mineralized (%)
Incubation time (h)

**Figure 2**

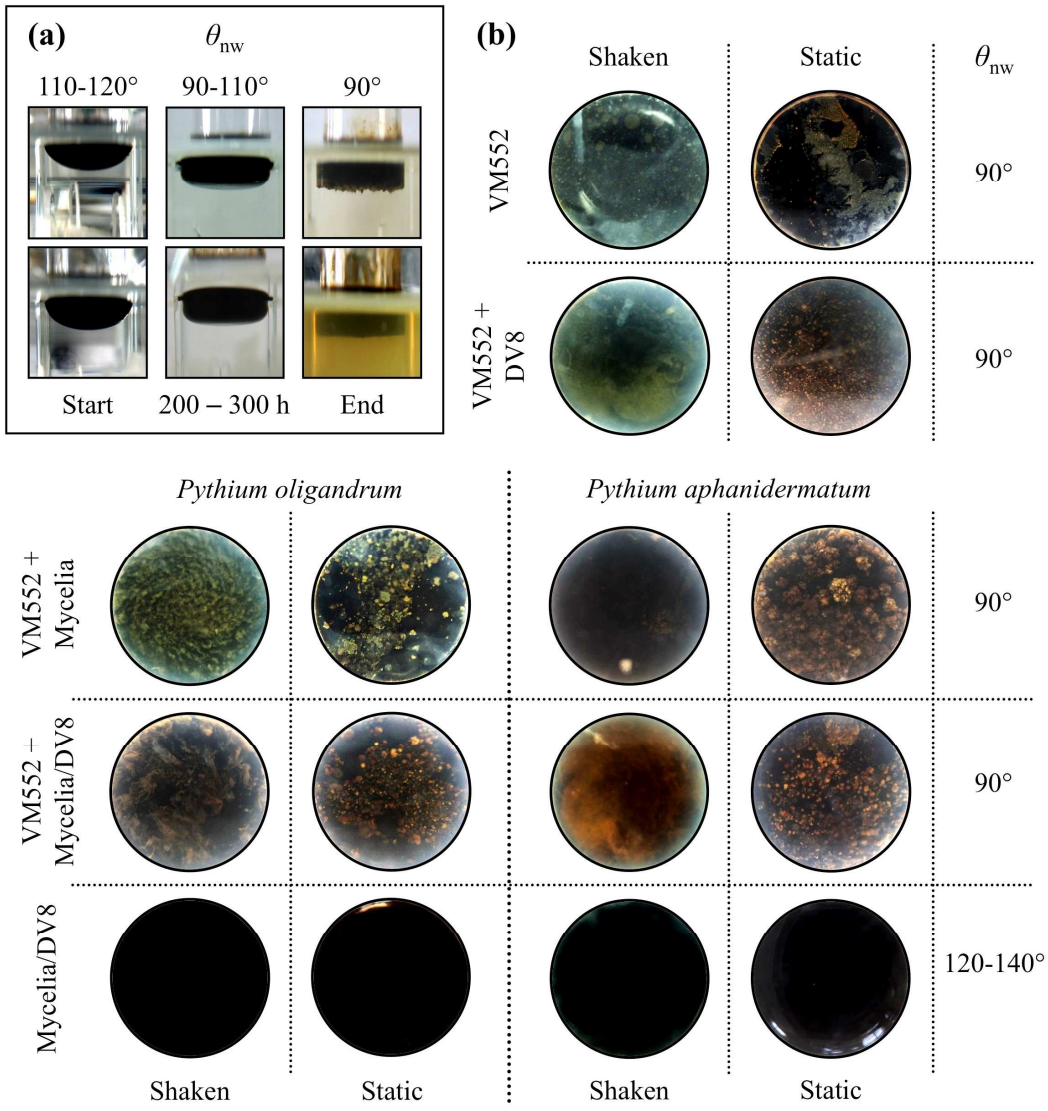
(a)
$\theta_{nw}$
110-120°
90-110°
90°
Start
200 – 300 h
End
(b)
Shaken
Static
$\theta_{nw}$
VM552
90°
VM552 + DV8
90°
Pythium oligandrum
Pythium aphanidermatum
VM552 + Mycelia
90°
VM552 + Mycelia/DV8
90°
Mycelia/DV8
120-140°
Shaken
Static
Shaken
Static